Journal of Power Sources 221 (2013) 28–34

Contents lists available at SciVerse ScienceDirect

Journal of Power Sources

journal homepage: www.elsevier.com/locate/jpowsour

Accelerated devitrification of a strontiumlanthanumaluminoborosilicate based intermediate temperature solid oxide fuel cell glass sealant and its effect on thermophysical behaviour of the glass ceramics

Prasanta Kumar Ojha [a,b,*], T.K. Chongdar [a], N.M. Gokhale [a], A.R. Kulkarni [b]

[a] Naval Materials Research Laboratory, Addl. Ambernath, Thane 421506, Maharashtra, India
[b] Indian Institute of Technology Bombay, Mumbai, India

HIGHLIGHTS

- Devitrification of a strontiumlanthanumaluminoborosilicate glass was investigated.
- Change in properties of the glass was correlated with the evolution of phases.
- With evolution of $SrAl_2Si_2O_8$ phase, CTE of the glass ceramics increases.
- With evolution of $La_{10}(SiO_4)_6O_3$ phase, CTE of the glass ceramics decreases.
- Even on 100 h devitrification at 1000 °C the glass ceramics is suitable for SOFC.

ARTICLE INFO

Article history:
Received 30 April 2012
Received in revised form
12 July 2012
Accepted 31 July 2012
Available online 13 August 2012

Keywords:
Glass sealant
Devitrification
Thermochemical stability
Intermediate temperature solid oxide fuel cell (IT-SOFC)

ABSTRACT

A strontiumlanthanumaluminoborosilicate based intermediate temperature solid oxide fuel cell (IT-SOFC) glass sealant has been investigated for isothermal devitrification under accelerated conditions. Sintering of the glass up to 100 h at 1000 °C, results in the formation of two crystalline phases evidenced by X-ray diffraction (XRD) analysis. Hexacelsian phase evolves from the initial hours of sintering; however, lanthanum silicate phase appears at longer hours of sintering. Quantitative XRD of the glass ceramics reveals that hexacelsian occupies majority of the crystalline phases and lanthanum silicate is occupying minor quantity. Formation of crystalline phases has been reconfirmed by microstructure analysis of glass ceramics through Scanning Electron Microscopy (SEM) and elemental analysis of phases by energy dispersive spectroscopy (SEM-EDS). Crystalline phases in the glass ceramics have been quantified by analysis of SEM images through Imagepro plus software. At different stages of sintering, CTE of the glass ceramics has been measured by dilatometer. Correlation of CTE with crystalline phases in the glass ceramics indicates that with formation of hexacelsian phase CTE of the glass ceramics increases, however, formation of lanthanum silicate phase reduces the CTE of the glass ceramics. Phase property correlation indicates that after 100 h of accelerated devitrification at 1000 °C, the glass ceramics attains phase stability therefore the CTE stabilizes and the value remains well within the requirement limit of SOFC sealant.

1. Introduction

In recent years, solid oxide fuel cell (SOFC) has emerged as one of the most challenging energy conversion technology because of its higher efficiency compared to other concurrent technologies, environment friendly nature and fuel flexibility. An SOFC cell has three major components a porous anode, dense electrolyte and a porous cathode. A single cell can generate at most several watt of power; thereby to generate high power output several such cells are stacked together. An SOFC stack can have two basic designs, planar and tubular. Out of which the planar design (pSOFC) provides greater power density compared to a tubular design because of the linear path of current flow [1–6]. Among the planar designs, anode supported planar design has been adopted by most of the leading SOFC developers that can be operated in an intermediate temperature range between 700 and 800 °C (IT-SOFC) [7,8]. Because of a comparatively low temperature operation,

* Corresponding author. Naval Materials Research Laboratory, Addl. Ambernath, Thane 421506, Maharashtra, India. Tel.: +91 251 2623219; fax: +91 251 2623004.
E-mail address: pkojha77@yahoo.co.in (P.K. Ojha).

0378-7753/$ – see front matter © 2012 Elsevier B.V. All rights reserved.
http://dx.doi.org/10.1016/j.jpowsour.2012.07.110

ceramic interconnect can be replaced by metallic interconnect and other operational costs can be reduced. Moreover, low temperature operation makes it easier to handle the cell component materials and delays the ageing of the materials thereby increases average life span of the cell. Despite all these advantages, a planar IT-SOFC stack requires gas tight sealant to provide edge sealing at SOFC operational temperature. The health of an SOFC stack grossly depends upon the long term thermophysical and thermochemical stability of the sealant in SOFC condition. Hence, selection of a proper sealant material is very important for fuel cell performance. For use in pSOFC, a sealant material should have low leakage of fuel/oxidant gas, optimum viscosity, good wettability, chemical inertness, and thermal expansion matching with adjacent SOFC components. In this regard, researchers have tried out several materials for SOFC sealant and all these materials can be broadly classified into three categories: compressive seals, compliant seals and rigid bonded seals [9–14]. Glass and glass ceramics as rigid bonded seals have advantages over other seals and are therefore preferred for SOFCs. For use in SOFC, a glass sealant should be chemically stable in both oxidizing and wet reducing conditions. CTE should be close to $10 \times 10^{-6}\,^{\circ}C^{-1}$. Glass transition temperature should be less than cell operating temperature and glass softening temperature high enough to maintain viscosity at cell operating temperature. Further, continuous and/or excessive devitrification of the glass should not occur during cell operation temperature.

Thermal stress in pSOFC is commonly observed due to mismatch of coefficient of thermal expansion (CTE) of glass with cell components and temperature gradient during operation. This has been recognized as criteria in selecting the seal materials [15–19]. Some glass systems rarely crystallize at high temperatures so that they overflow due to lowering of viscosity at SOFC operational temperature. Others may partly or completely crystallize during high temperature operation. Crystallization of a glass mainly depends on the glass composition and thermal history of the sample. Crystallization in glass seals is reported to show better physical properties but it causes serious CTE mismatch [9,19,20] which affects the cell performance. For a glass to be used as rigid seal in pSOFC, it must have CTE matching with other SOFC components for a longer period of operation. Thus, flowability and crystallization of glass sealants are two important factors related to thermal stress distribution and mechanical integration in pSOFC stack. The glass sealant should have controlled crystallization and the crystalline phases should be stable so that the sealant can be used for longer time.

Considering all these factors, researchers have tried out several glasses and glass ceramics based on borates, phosphates and silicates and studied their compatibility with both cell components and interconnect [12,21–30]. Out of all these candidate glasses borosilicate glasses with proper B_2O_3/SiO_2 ratio are best suited for SOFC sealing application [23,31,32]. Again, La_2O_3 as a modifier in the glass composition controls the viscosity of the glass sealant at SOFC operational condition [23]. SrO modifies the CTE [33] and Al_2O_3 retards devitrification [34].

Therefore we have selected a group of $SrO–La_2O_3–Al_2O_3–B_2O_3–SiO_2$ based glasses and have investigated their thermal and physical properties to evaluate their suitability as SOFC sealant [35,36]. The research work in this article is an extension of the previous work reported elsewhere [36]. In this work the glass has been investigated for its long term thermochemical and thermophysical stability.

As mentioned in the previous report [36], thermal properties of the glass make it suitable for IT-SOFC application in an operating temperature range 700–800 °C, however, the glass shows two crystallization temperatures under differential scanning calorimetric (DSC) at 807 °C and at 1021 °C. As mentioned previously that devitrification in glass sealant leads to a drastic change in the CTE which is undesired for SOFC application. Therefore in this piece of work, devitrification of the strontiumlanthanumaluminoborosilicate glass has been investigated and corresponding change in the CTE is evaluated. The devitrification in the glass has been carried out at an elevated temperature compared to SOFC operating temperature. The glass has been systematically heat treated at 1000 °C up to 100 h and the phase formation process has been evaluated by XRD and SEM analysis. In each step of devitrification, the CTE of the glass ceramics has been measured through dilatometer. An effort has been made to establish a phase property correlation between the phases formed in the glass ceramics and CTE of it, which highlights the importance of the work.

2. Experimental

A glass with composition SrO (25.7 mol %), La_2O_3 (4.1 mol %), Al_2O_3 (13.1 mol %), B_2O_3 (12.8 mol %) and SiO_2 (44.3 mol %) was heat treated from 700 °C to 1000 °C at an interval of 100 °C. At each temperature the glass was sintered for 15 min. Similarly, the glass was heat treated at 1000 °C for different time up to a maximum of 100 h. At 1000 °C the glass was heat treated for 2 h, 5 h, 10 h, 15 h, 25 h, 50 h and 100 h. In each case the sample was heated from room temperature to the sintering temperature at a heating rate of 5 °C min^{-1}. The sample was hold at the temperature for desired time and was cooled to room temperature by air cooling. All the characterizations of heat treated samples were carried out at room temperature.

Phase analysis of heat treated samples were carried out by powder X-ray diffraction (XRD) using XPert MPD, PAnalytical model, Philips, Netherlands. For phase identification and quantification of phases, semi-quantitative Rietveld method was used.

Scanning Electron Microscopy (SEM) (LEO 1455, UK) was used at room temperature to analyze the microstructures of base glass and heat treated glasses. The compositions of crystalline phases were determined using energy dispersive spectroscopy (SEM-EDS).

SEM images were analyzed through 'Imagepro plus' software for quantitative analysis of phases. Through this software each phase was assigned with a particular color code and was analyzed to get phase details. A calibrated scale was used to obtain grain size, aspect ratio and percentage of crystallinity for each phase. Grain details were obtained from the average data of 50 numbers of grains. Percentage of crystallinity was calculated from area occupied by the crystalline phase with respect to the total area of the glass ceramics.

Coefficients of thermal expansion (CTE) of the heat treated glass samples were measured using a vertical push rod type UNITHERM™ MODEL 1161 Dilatometer System made by Anter Corporation, USA. Through dilatometer, percentage of linear expansion of the sample was measured as a function of temperature. CTE of the sample was calculated using slope of the expansion plot and sample dimension.

3. Results and discussion

In the previous report [36] the glass was thoroughly characterized for its physical and thermal behaviour. In that report, amorphous nature of the glass was evident from X-ray diffraction. Thermal characterization of the glass was carried out by differential scanning calorimetry (DSC). Through DSC it was observed that the glass undergoes glass transition (T_g) at 625 °C and on heat treatment two crystallization phases (T_p) evolve out of the glass matrix at 807 °C and at 1021 °C. Through dilatometric analysis characteristic temperatures were measured for bulk glass and found to be: glass transition temperature (T_g) at 644 °C and glass softening

temperature (T_s) at 709 °C. Coefficient of thermal expansion (CTE) of the glass was calculated using the expansion data from dilatometer and found to be 9.72×10^{-6} °C^{-1}. The glass was thoroughly investigated for other properties and found suitable for its application as sealant in IT-SOFC at an operational temperature of 700–800 °C.

In the present study, the base glass has been investigated for its thermochemical stability up to 100 h at 1000 °C. And, the effect of devitrification on the thermophysical behaviour of the glass ceramics has been reported. To investigate the thermochemical stability, the glass was heat treated at different temperatures as mentioned in the experimental section. On heat treatment, the devitrification of the glass was investigated by XRD and SEM-EDS. Crystalline phases were quantified by analysing the SEM images using Imagepro plus software. CTE of the heat treated glass was measured by dilatometer and was correlated with the phases formed on heat treatment.

As mentioned in the experimental section, the base glass was heat treated at 700, 800, 900 and 1000 °C for 15 min each. Powder XRD was carried out at room temperature for each such heat treated glass sample and results are shown in Fig. 1. From the figure it was observed that diffractogram of glass sample heat treated at 700 °C shows no significant peak and is similar to the neat glass [36]. This may be due to heat treatment at 700 °C is not thermodynamically sufficient for devitrification of the glass and it remains free of crystallinity. X-ray diffractogram of glass heat treated at 800 °C shows low intensity peaks which indicate emergent of crystalline phases out of the glass, however, the percentage of crystallinity may be less. The findings for glass heat treated at 700 and 800 °C agree with the DSC data which showed the appearance of first crystallization peak at 807 °C [36]. Diffractograms of glass heat treated at 900 °C and 1000 °C showed high intensity peaks indicative of the increased crystallinity in the matrix. To identify crystalline phases ascribing to these peaks, all three diffractograms of glass heat treated at 800, 900 and 1000 °C were analyzed through semi-quantitative analysis. Phase analysis revealed that in all three diffractograms, peaks represent the same crystalline phase and the phase was identified to be hexacelsian ($SrAl_2Si_2O_8$). This indicates that devitrification of the glass initiates at 800 °C with appearance of peaks in the XRD spectrum and the crystallization process gets accelerated at 1000 °C resulting high intensity peaks in the XRD spectrum.

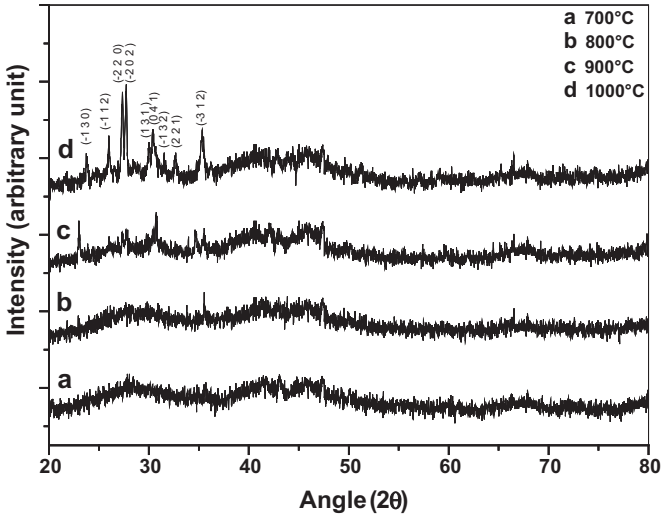

Fig. 1. XRD of the glass heat treated at different temperatures.

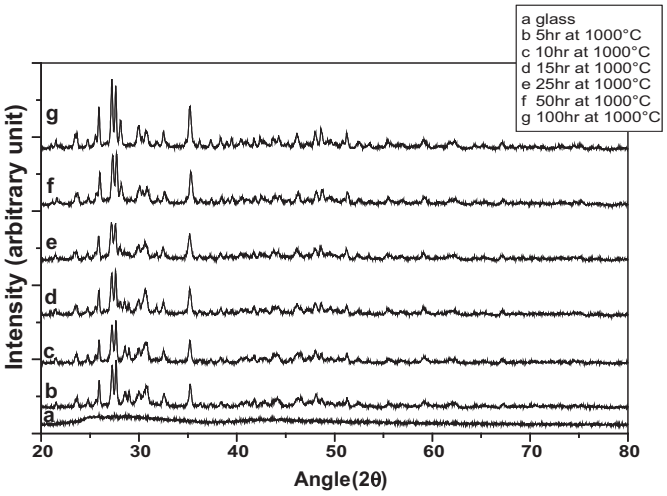

Fig. 2. XRD of the glass heat treated at 1000 °C for different time.

Glass samples were heat treated at 1000 °C for 5, 10, 15, 25, 50 and 100 h. The heat treated samples were characterized at room temperature using powder XRD and results are shown in Fig. 2. Figure shows that diffractograms of all samples carry high intensity peaks, which indicate the presence of well-defined crystalline phases in the heat treated glass matrix. Peaks observed in the XRD plots were indexed and phases were identified. On phase analysis it was observed that diffractograms of 5 and 10 h sintered glass samples have only hexacelsian phase peaks in the spectrum, however, phase peaks of a second crystalline phase are present in the spectrum of glass samples sintered for 15 h and more. On phase analysis the second phase found to be lanthanum silicate, $La_{10}(SiO_4)_6O_3$. It was confirmed from XRD that even after 100 h of sintering at 1000 °C, the glass ceramics shows no new phase formation, and confine to these two crystalline phases only. As shown in Fig. 3, crystalline phases were quantified for 100 h heat treated glass ceramics and it was found that hexacelsian phase occupies 90 volume% of the total crystallinity with 10 volume% lanthanum silicate phase.

To analyze the microstructures, SEM images were generated for all the heat treated glass samples. Fig. 4 shows the SEM microstructures of the base glass and glass sintered at 700, 800, 900 and 1000 °C for 15 min each. From the figure it is evident that microstructure of glass heat treated at 700 °C is similar to the

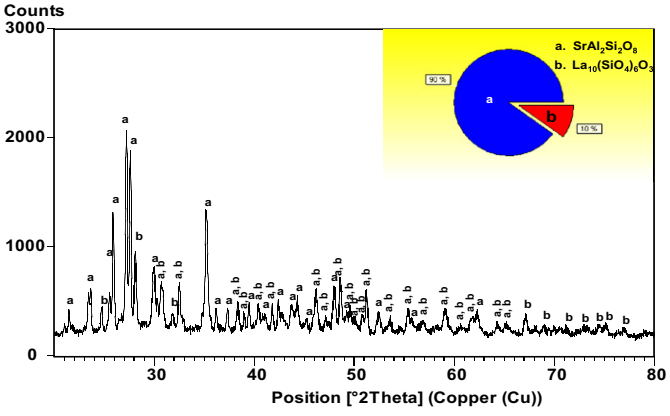

Fig. 3. Phase analysis from the XRD pattern of the glass heat treated at 1000 °C for 100 h.

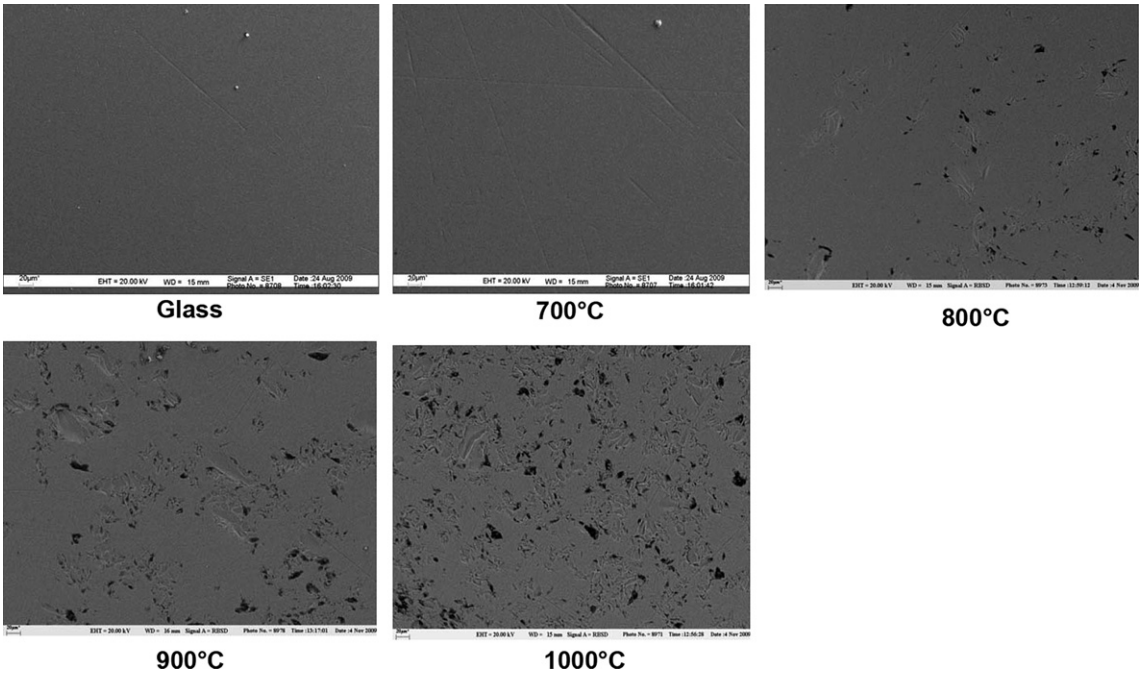

Fig. 4. SEM images of glass heat treated at different temperatures.

microstructure of base glass with no evidence of crystalline phase. Microstructures of glasses sintered at 800, 900 and 1000 °C show a systematic conversion of the base glass into a glass ceramics with appearance of crystalline phases. Elemental analysis of crystalline phases through SEM-EDS confirmed them to be hexacelsian ($SrAl_2Si_2O_8$) phases. It was observed from the microstructures that with increase in temperature the number of nucleation sites increased and sizes of the nuclei grew bigger. This result is in congruent with the XRD analysis, which showed the evolution of hexacelsian phase during this temperature range.

SEM microstructures of glass heat treated at 1000 °C for 5, 10, 15, 25, 50 and 100 h are shown in Fig. 5. Microstructure shows that within 5 h of sintering at 1000 °C, the glass is turned into a glass ceramics with well-developed needle shaped hexacelsian ($SrAl_2Si_2O_8$) crystalline phases. Up to 10 h of sintering hexacelsian found to be the only crystalline phase in the glass ceramics. SEM images of glass samples sintered for 15 h and more show a second crystalline phase in the glass matrix along with the original hexacelsian phase. The second phase grains are smaller in numbers and sizes which occupied a very small fraction of the total volume. Elemental

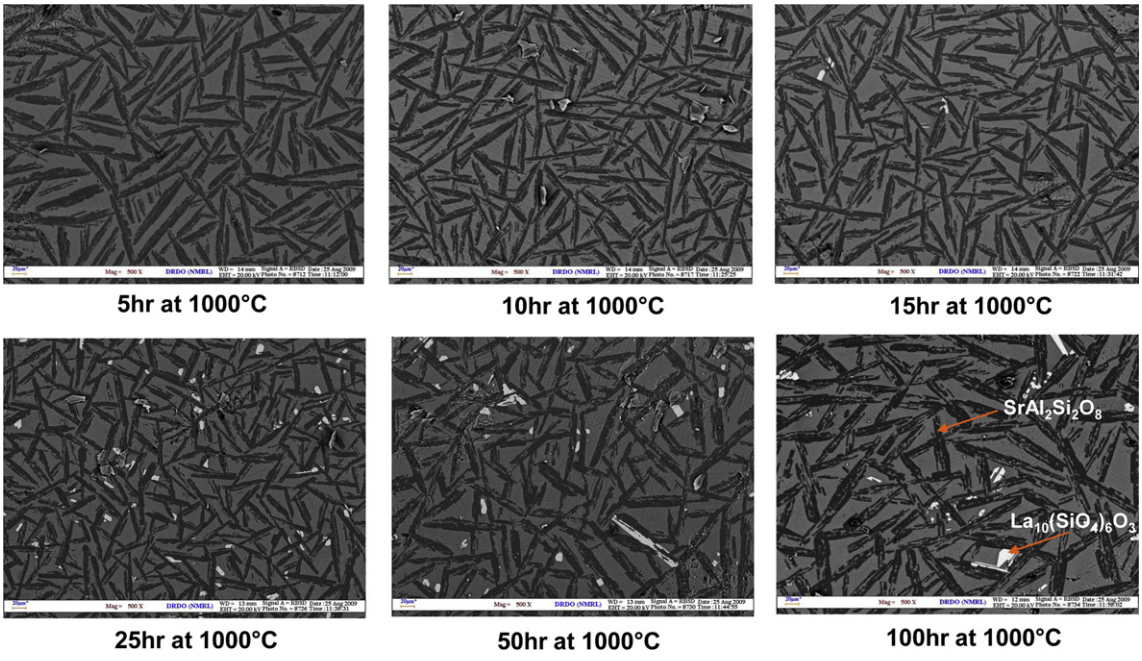

Fig. 5. SEM images of glass heat treated at 1000 °C for different time.

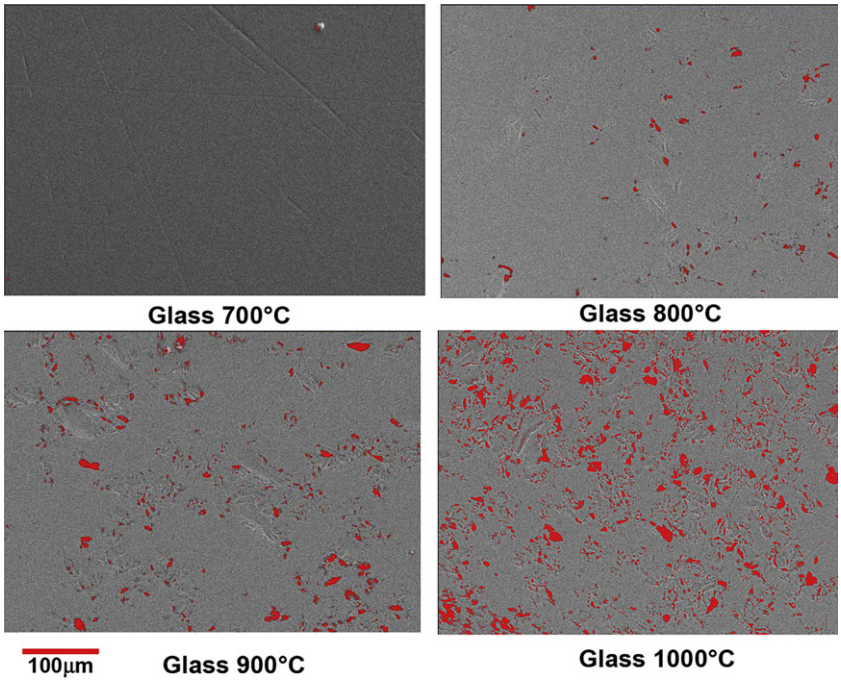

Fig. 6. Image analysis of SEM microstructures of the glass heat treated at different temperatures.

analysis by SEM-EDS shows it to be lanthanum silicate phase. Again, this observation is consistent with the findings from XRD, which showed the growth of lanthanum silicate phase on sintering for 15 h and more at 1000 °C.

For quantitative analysis of phases, all the SEM microstructures were analyzed using Imagepro plus software. Figs. 6 and 7 show the analyzed SEM images, where different phases have been assigned with different colors: glass matrix with grey color, hexacelsian with red and lanthanum silicate with white color. Data generated by image analysis are enlisted in Table 1. The results show that at 700 °C there is no crystalline phase. At 800 °C the hexacelsian phase occupies a volume fraction of 0.6% of the glass ceramics. Data indicates that heat treatment of the glass from 800 to 1000 °C leads to increase in crystallinity from 0.6 to 3.2 volume%, however, significant increase in crystallinity is observed upon sintering for 5 h at 1000 °C. Glass sintered for 5 h at 1000 °C shows a total crystallinity of 56 volume%. Subsequent to that, in next 5 h of sintering volume of hexacelsian increased by 1% only and remains stable at 57 volume% for next 90 h. Results in Table 1 show that the second phase, lanthanum silicate occupies a very small volume fraction in the glass ceramics matrix. The phase growth initiates at 15 h of sintering at 1000 °C. At this point lanthanum silicate

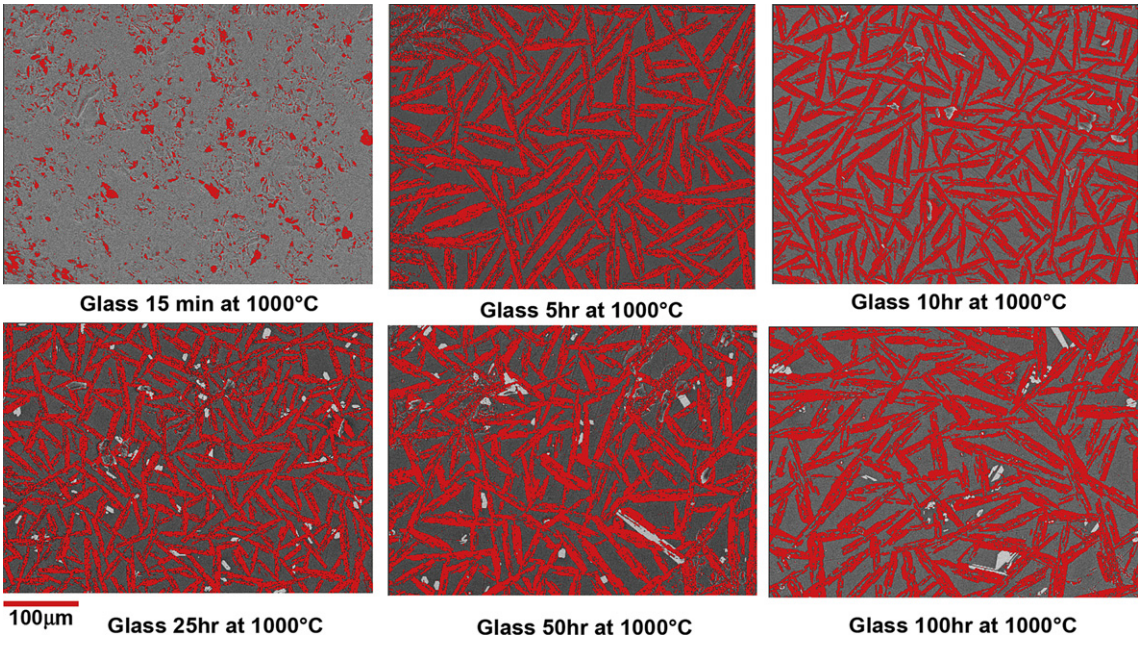

Fig. 7. Image analysis of SEM microstructures of the glass heat treated at 1000 °C for different time.

Table 1
Quantitative data generated from image analysis of the SEM microstructures of heat treated glass samples.

Specification of the sample	Crystalline phase analysis								
	Crystal grain details ($SrAl_2Si_2O_8$)				Crystal grain details ($La_{10}(SiO_4)_6O_3$)				Total
	Length (μm)	Width (μm)	Aspect ratio	Crystallinity (%)	Length (μm)	Width (μm)	Aspect ratio	Crystallinity (%)	Crystallinity (%)
Room temperature	–	–	–	–	–	–	–	–	0
700 °C 15 min	–	–	–	–	–	–	–	–	0
800 °C 15 min	7.6	4.4	1.8	0.6	–	–	–	–	0.6
900 °C 15 min	12.5	6.6	2	1.8	–	–	–	–	1.6
1000 °C 15 min	11.2	6.4	1.9	3.2	–	–	–	–	3.2
1000 °C 5 h	80	15	6.4	56	–	–	–	–	56
1000 °C 10 h	69	12	7	57	–	–	–	–	57
1000 °C 15 h	59	11	6.8	57	10	4.7	2.1	0.1	57.1
1000 °C 25 h	51	9.5	6.3	57	12	5.2	2.3	2	59
1000 °C 50 h	78	15	6	57	14	7	2	5	62
1000 °C 100 h	97	18	6.5	57	12	5.5	2	5	62

contributes to 0.1 volume% of the total glass ceramics matrix, however, the volume fraction increases with sintering time and it occupies a total volume fraction of 2% on 25 h sintering at 1000 °C. On 50 h of sintering the volume fraction increases to 5% and remains constant there after up to 100 h of sintering. After 100 h of sintering, hexacelsian phase occupies 57 volume% and lanthanum silicate 5 volume % of the glass ceramics. Again both these phases stabilize by their volume thereby the total crystallinity in the glass ceramics stabilizes to 62 volume % with remaining 38% glass. That indicates a positive sign that after 100 h of devitrification at 1000 °C the glass shows a thermochemical stabilization. However, to investigate the corresponding changes in the thermophysical behaviour of the glass due to devitrification, its CTE was measured via dilatometric analysis. In each step of devitrification the sintered glass sample was undertaken through dilatometer to measure the linear thermal expansion vs. temperature and CTE was calculated out of it. Linear expansion of glass ceramics as a function of temperature is shown in Fig. 8. Figure carries a level indicative of the thermal history of each sample. In this experiment a glass sintered for 2 h at 1000 °C was added extra and its expansivity was measured and reported. Again, linear expansion curves for yttria stabilized zirconia (8YSZ) (SOFC electrolyte) and ferritic steel (SOFC interconnect) are also shown in the same figure for comparison. The CTE values were calculated from the expansion data using sample dimensions and values are presented in Table 2 along with the thermal history of the sample and volume fraction of different phases in the glass ceramics as derived from the SEM image analysis.

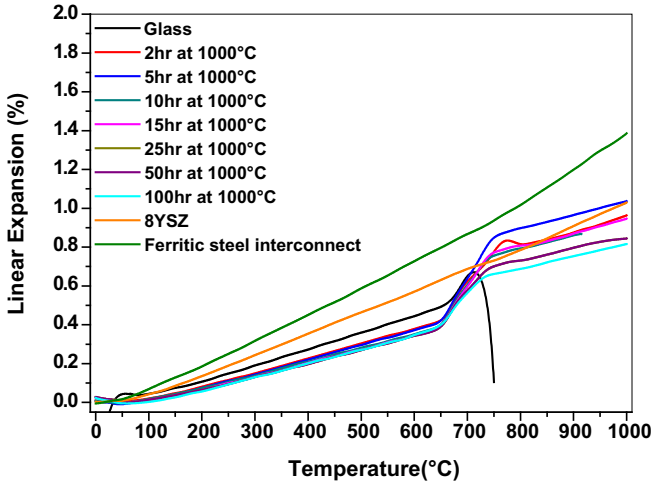

Fig. 8. Linear expansion of heat treated glass samples, 8YSZ and steel interconnect at different temperatures.

Data shows that CTE of the base glass is $9.7 \times 10^{-6}\,°C^{-1}$ and that of 8YSZ and ferritic steel are $10.1 \times 10^{-6}\,°C^{-1}$ and $11.1 \times 10^{-6}\,°C^{-1}$, respectively, at 800 °C. On accelerated crystallization at 1000 °C, the CTE of the glass ceramics varies significantly. After 2 h of sintering at 1000 °C, the CTE of the glass increased suddenly from 9.7 to $11.1 \times 10^{-6}\,°C^{-1}$. After 5 h it increased further to attain the maximum value of $11.7 \times 10^{-6}\,°C^{-1}$. On further sintering, CTE started decreasing. Sample sintered for 15 h at 1000 °C shows a CTE of $10.6 \times 10^{-6}\,°C^{-1}$. After 25 h of sintering, CTE of the glass ceramics decreased significantly to $9.6 \times 10^{-6}\,°C^{-1}$ and it attained a value of $9.4 \times 10^{-6}\,°C^{-1}$ after 50 h of sintering. After 100 h of sintering at 1000 °C glass ceramics attained a CTE value of $9.1 \times 10^{-6}\,°C^{-1}$.

The variation of CTE of the glass ceramics may be explained on the basis of evolution of different crystalline phases and quantity of each phase at various stages of sintering. As discussed previously, two crystalline phases evolve out of the glass on heat treatment, i) hexacelsian, ii) lanthanum silicate. From literature it was found that CTE of hexacelsian is $10.6 \times 10^{-6}\,°C^{-1}$ [37] and that of $La_{10}(SiO_4)_6O_3$ is $9.7 \times 10^{-6}\,K^{-1}$ [38]. In this case of devitrification of the strontiumlanthanumaluminoborosilicate glass, in the initial hours of heat treatment the hexacelsian phase is evolved in the glass matrix which leads to an increase in the CTE of the glass ceramics. On further sintering, the CTE decreases with emergence of lanthanum silicate phase. However, to establish an exact correlation between volume of various phases present in the glass ceramics and the CTE of the glass ceramics is difficult as with formation of crystalline phases, the composition of the remaining glass matrix changes thereby its CTE may be changing. In fact it needs to carry out a further detailed analysis between different phases present in the

Table 2
CTE of sintered glass samples with their thermal history and various phases present in the glass ceramics along with CTE of 8YSZ and ferritic steel interconnect.

Thermal history of sample	Volume % of different phases in the glass-ceramics			CTE ($\times 10^{-6}\,°C^{-1}$)
	Glass	$SrAl_2Si_2O_8$	$La_{10}Si_6O_{27}$	
Ferritic steel				11.1 (at 800 °C)
8YSZ				10.1 (at 800 °C)
Glass	100			9.7
Glass-2 h 1000 °C	–			11.1
Glass-5 h 1000 °C	44	56		11.7
Glass-10 h 1000 °C	43	57		11.1
Glass-15 h 1000 °C	42.9	57	0.1	10.6
Glass-25 h 1000 °C	41	57	2	9.6
Glass-50 h 1000 °C	38	57	5	9.4
Glass-100 h 1000 °C	38	57	5	9.1

glass ceramics and their contribution towards thermal expansion of the matrix using the standard additive rule [39]:

$$\alpha = \sum_i m_i \alpha_i + a \quad (1)$$

where α is the CTE of the glass ceramics, m_i and α_i are mole fraction and CTE of each phase present in the matrix and a_i is a constant factor for phase i.

For application in SOFC, CTE of seal glass should match with those of other SOFC components so as to avoid thermal stress. When there is a CTE difference, both tensile (for $CTE_{component} > CTE_{glass}$) and compressive (for $CTE_{component} < CTE_{glass}$) stresses are possible at the interface [40,41]. To avoid thermal stress CTE difference should be within $1 \times 10^{-6}\,^{\circ}C^{-1}$ [42]. Tensile stress often leads to cracks at the interface in the glass. Compressive stress to some extent can be tolerated because the compressive strength of a seal glass is much higher than the tensile strength (as high as 15 times [43]). But excessive compressive stress causes delamination of the glass from the interfacing SOFC components. Thermal stress σ due to the CTE mismatch between the seal glass and the specific cell component can be expressed as [44]:

$$\sigma = CE \int_{T_Q}^{T_R} (\alpha_g - \alpha_c) dT \quad (2)$$

where C is a geometrical constant, E is Young's modulus of the seal glass, α_g and α_c are the CTEs of the glass and the cell component under consideration, T_Q is the set point temperature for the glass, and T_R is the room temperature. In this case, the glass after 100 h accelerated devitrification at 1000 °C shows phase stability and the CTE stabilizes to $9.1 \times 10^{-6}\,^{\circ}C^{-1}$ which is well within $\pm 1 \times 10^{-6}\,^{\circ}C^{-1}$ of SOFC component, hence suitable for SOFC sealant.

4. Conclusions

A SrO (25.7 mol %), La_2O_3 (4.1 mol %), Al_2O_3 (13.1 mol %), B_2O_3 (12.8 mol %) and SiO_2 (44.3 mol %) based IT-SOFC glass sealant was investigated for accelerated devitrification at 1000 °C. It was evident from XRD analysis that devitrification of glass with evolution of hexacelsian phase initiates at 800 °C and gets accelerated at 1000 °C. Sintering of the glass at 1000 °C for different hours showed the development of two crystalline phases in the glass matrix, major hexacelsian phase ($SrAl_2Si_2O_8$) and secondary lanthanum silicate ($La_{10}(SiO_4)_6O_3$) phase which appeared only after 15 h of sintering. After 100 h of sintering both the phases stabilized by volume with hexacelsian occupying 57 volume% of the total glass ceramics and lanthanum silicate of 5 volume%. Thereby, the glass ceramics attained thermochemical stability with a residual 38 volume% of glass in the matrix. Evolution of both crystalline phases led to thermophysical instability in the glass system. With evolution of hexacelsian phase the CTE of the glass ceramics increased significantly compared to base glass of $9.7 \times 10^{-6}\,^{\circ}C^{-1}$. Up to 15 h of sintering CTE of glass ceramics passed through a maximum of $11.7 \times 10^{-6}\,^{\circ}C^{-1}$ and attained a value of $10.6 \times 10^{-6}\,^{\circ}C^{-1}$ at 15 h of sintering. Beyond this, sintering of the glass resulted in the formation of the lanthanum silicate phase along with the hexacelsian phase thereby the CTE of the glass ceramics decreased suddenly to $9.6 \times 10^{-6}\,^{\circ}C^{-1}$at 25 h of sintering. After 50 h of sintering both the crystalline phases stabilized in the glass ceramics, therefore, CTE of the glass ceramics also stabilized and after 100 h of sintering the glass ceramics attained a CTE value of $9.1 \times 10^{-6}\,^{\circ}C^{-1}$.

References

[1] N.Q. Minh, Solid State Ionics 174 (2004) 271–277.
[2] S.C. Singhal, Solid State Ionics 152-153 (2003) 405–410.
[3] N.Q. Minh, J. Am. Ceram Soc. 76 (3) (1993) 563–588.
[4] B.C.H. Steele, A. Heinzel, Nature 414 (6861) (2001) 345–352.
[5] S.P.S. Badwal, Solid State Ionics 143 (1) (2001) 39–46.
[6] L.J. Gauckler, D. Beckel, B.E. Buergler, E. Jud, U.P. Muecke, M. Prestat, Chimia 58 (12) (2004) 837–850.
[7] S. Singhal, K. Kendall, High Temperature Solid Oxide Fuel Cells: Fundamental, Design and Applications, Elsevier, UK, 2003.
[8] R.N. Basu, G. Blass, H.P. Buchkremer, D. Stöver, F. Tietz, E. Wessel, I.C. Vinke, J. Eur. Ceram. Soc. 25 (4) (2005) 463–471.
[9] J.W. Fergus, J. Power Sources 147 (2005) 46–57.
[10] P.A. Lessing, J. Electrochem. Soc. 42 (2007) 3465–3476.
[11] R.N. Singh, Int. J. Appl. Ceram. Technol. 4 (2007) 134–144.
[12] Ira D. Bloom, Kevin L. Ley, U.S. Patent (1995) 5,453,331.
[13] Tsung Leo Jiang, Ming-Hong Chen, Int. J. Hydrogen Energy 34 (2009) 8223–8234.
[14] K.S. Weil, B.J. Koeppel, J. Power Sources 180 (2008) 343–353.
[15] N. Govindaraju, W.N. Liu, X. Sun, P. Singh, R.N. Singh, J. Power Sources 190 (2009) 476–484.
[16] C.S. Montross, H. Yokokawa, M. Dokiya, Br. Ceram. Trans. 101 (2002) 85–93.
[17] A. Atkinson, B. Sun, Mater. Sci. Technol. 23 (2007) 1135–1143.
[18] C.-K. Lin, T.-T. Chen, Y.-P. Chyou, L.-K. Chiang, J. Power Sources 164 (2007) 238–251.
[19] C.-K. Lin, L.-H. Huang, L.-K. Chiang, Y.-P. Chyou, J. Power Sources 192 (2009) 515–524.
[20] K.D. Meinhardt, D.-S. Kim, Y.-S. Chou, K.S. Weil, J. Power Sources 182 (2008) 188–196.
[21] W. Liu, X. Sun, M.A. Khaleel, J. Power Sources 185 (2008) 1193–1200.
[22] K.D. Meinhardt, J.D. Vienna, T.R. Armstrong, L.R. Pederson, U.S. Patent (2003) 6,532,769.
[23] K.L. Ley, M. Krumpelt, R. Kumar, J.H. Meiser, I. Bloom, J. Mater. Res. 11 (6) (1996) 1489–1493.
[24] S.-B. Sohn, S.-Y. Choi, G.-H. Kim, H.-S. Song, G.-D. Kim, J. Am. Ceram. Soc. 87 (2004) 254–260.
[25] R.E. Loehman, H.P. Dumm, H. Hofer, Ceram. Eng. Sci. Proc. 23 (2002) 699–705.
[26] K. Eichler, G. Solow, P. Otschik, W. Schaffrath, J. Eur. Ceram. Soc. 19 (1999) 1101.
[27] P. Geasee, R. Conradt, T. Schwickert, A. Janke, J. Remmel, F. Tietz, In: Proc. Int. Congr. Glass, vol. 2 (2001) 47 (extended abstracts).
[28] R. Zheng, S.R. Wang, H.W. Nie, T.-L. Wen, J. Power Sources 128 (2004) 165–172.
[29] Z. Yang, K.D. Meinhardt, J.W. Stevenson, J. Electrochem. Soc. 150 (2003) A1095–A1101.
[30] Z. Yang, J.W. Stevenson, K.D. Meinhardt, Solid State Ionics 160 (2003) 213–225.
[31] P.H. Larsen, C. Bagger, M. Mogensen, J.G. Larsen, In: Proc. 4th Int. Symp. Solid Oxide Fuel Cells 95(1) (1995): 69–78.
[32] C. Gunther, G. Hofer, W. Kleinlein, In: Proc. 5th Int. Symp. Solid Oxide Fuel Cells 97(18) (1997): 746–756.
[33] M.B. Volf, Chemical Approach to Glass, Glass Sci Tech, vol. 7, Elsevier, New York, 1984.
[34] J.H. Jean, T.K. Gupta, J. Mater. Res. 8 (1993) 356–363.
[35] P.K. Ojha, S.K. Rath, T.K. Chongdar, N.M. Gokhale, A.R. Kulkarni, J. Power Sources 196 (2011) 4594–4598.
[36] P.K. Ojha, T.K. Chongdar, N.M. Gokhale, A.R. Kulkarni, Int. J. Hydrogen Energy 36 (2011) 14996–15001.
[37] Y. Kobayashi, M. Inagaki, J. Eur. Ceramic Soc. 24 (2004) 399–404.
[38] S.P. Jiang, L. Zhanga, H.Q. Hea, R.K. Yapa, Y. Xiang, J. Power Sources 189 (2009) 972–981.
[39] M.B. Volf, Glass Science and Technology, Elsevier, Amsterdam, 1984.
[40] I.W. Donald, J. Mat. Sci. 28 (1993) 2841–2886.
[41] I.W. Donald, B.L. Metcalfe, L.A. Gerrard, J. Am. Ceram. Soc. 91 (2008) 715.
[42] R. Kirsch, Glass Science and Technology, vol. 13, Elsevier, Amsterdam, 1993, p. 352.
[43] S. Linderoth, P.V. Hendriksen, M. Mogensen, J. Mater. Sci. 31 (1996) 5077.
[44] M. Mantel, J. Non-Cryst. Solids 273 (2000) 294.